



HAL
open science

Impact of the antenna topology on the combination of full-duplex spatial modulation and RF energy harvesting

Hery Zo Jean Baptiste Andriamanohisoa, Florin Doru Hutu, Guillaume Villemaud

► To cite this version:

Hery Zo Jean Baptiste Andriamanohisoa, Florin Doru Hutu, Guillaume Villemaud. Impact of the antenna topology on the combination of full-duplex spatial modulation and RF energy harvesting. Eucap 2024, Eurapp, Mar 2024, Glasgow, United Kingdom. hal-04492511

HAL Id: hal-04492511

<https://hal.science/hal-04492511>

Submitted on 6 Mar 2024

HAL is a multi-disciplinary open access archive for the deposit and dissemination of scientific research documents, whether they are published or not. The documents may come from teaching and research institutions in France or abroad, or from public or private research centers.

L'archive ouverte pluridisciplinaire **HAL**, est destinée au dépôt et à la diffusion de documents scientifiques de niveau recherche, publiés ou non, émanant des établissements d'enseignement et de recherche français ou étrangers, des laboratoires publics ou privés.

Impact of the antenna topology on the combination of full-duplex spatial modulation and RF energy harvesting

Hery Zo Andriamanohisoa, Florin-Doru Hutu, Guillaume Villemaud

Univ Lyon, INSA Lyon, INRIA, CITI, EA3720, 69621 Villeurbanne, France
hery-zo.andriamanohisoa@insa-lyon.fr

Abstract—In the context of full-duplex spatial modulation (FDSM) systems, this paper proposes a strategy that exploits the subset of antenna that is not used by the transmitter nor by the receiver to perform RF energy harvesting (RFEH). Through the mutual coupling effect, the transmitting antenna of each node transfers a part of its power to the other antennas of the array. Our idea is to recycle this power at this same node in complement to the ambient RF sources. Our study shows that the level of the available power may be greater than the RF ambient sources. The impact of the spacing d between the elements of an array of four antennas on the performance of the FDSM-RFEH was studied. For the RFEH aspect, when d is small, the harvested DC power level is greater. Contrary, for the FDSM aspect, when d is small, the level of the interference to noise ratio (INR) is greater, and the self-interference cancellation (SIC) is therefore impossible. The best compromise for the spacing is $d = 0.6\lambda$, where λ is the wavelength. By analysing the transfer coefficients extracted from S-parameters simulations performed on a four patch linear antenna array, the role of each antenna (emission, reception, RF energy harvesting) may be established.

Index Terms—Spatial modulation, Full-duplex, Energy harvesting, Mutual coupling

I. INTRODUCTION

Nowadays, with the Internet of Things (IoT) development, the number of connected devices grows spectacularly. Consequently, the energy consumption grows with the number of devices. To maintain the usability of the IoT, one should use a low energy consuming device. Moreover, the wireless spectrum resource employed in wireless communication is limited, so the reuse of the same resource to support different transmissions is necessary. The idea of a full-duplex (FD) communication is to use the same frequency band simultaneously in both directions (uplink and downlink). But to make full-duplex possible, one must manage the self-interference cancellation (SIC) issue.

In parallel, the use of the spatial modulation (SM) technique allows to reduce the energy consumption in a multi-antenna system [1]. SM is a recent MIMO technology that uses the active state of antennas as a support for the transmission of information. Unlike the other MIMO techniques, SM uses only one radio chain for all the emitting antennas. In [2], the performance of SM has been theoretically studied in terms of Average Bit Error Probability (ABEP). The authors gave

an analytical framework to study the performance of SM. In [3], the authors give a design guideline to implement the SM. They focused their studies on the associated transceiver design and on the spatial constellation optimization. To make the SM more attractive and more reliable, the authors in [4] proposed the implementation of the idea of full duplex in spatial modulation. The authors exploit the subset of antennas that is not used for the transmission to receive the signal from a remote node. An architecture with a SIC block via an appropriate algorithm has been proposed. In [5], the impact of the self-interference cancellation accuracy on the performance of the full-duplex spatial modulation (FDSM) was studied. Further, in [6], the performance of FDSM in the presence of IQ imbalance was studied by using Keysight ‘ADS software and MathWorks’s Matlab co-simulation.

Additionally, the energy harvesting using radio-waves is a way to recycle the energy lost in wireless communications. The idea is to convert the electromagnetic waves into electrical energy that can be stored or used to power supply a part of a circuit. In [7], the authors cite all the available ambient RF energy sources to operate energy harvesting. The power density available in the frequency range of 3 kHz - 3 GHz is detailed. In [8], the authors reviewed the evolution of electromagnetic energy conversion techniques over the years. The historical milestones and the breakthroughs on low-density energy harvesting are emphasised. In [9], the authors present the different possible topologies of an energy harvesting circuit. The efficiency of an energy harvesting circuit is the ratio between the power of the direct-current at its output and the power of the incoming RF signal. The efficiency of each topology is given according to the level of the available power and to the employed frequency. In [10], the authors give a review of the antenna technologies used for ambient RF energy harvesting (RFEH). The requirements in the antenna design for RFEH are developed more in details.

In [11], the authors propose a new way of considering the role of self-interference in wireless communications. They propose that one can exploit the SI in a positive manner, for instance as a source of energy. In [12], a system capable of amplify and forward relaying which uses FDSM is proposed. To ensure the power supply of the relay, it is equipped with

RFEH ability. However, the communication and the energy harvesting are not operated simultaneously. In this paper, we propose the study of the FDSM+RFEH combination, from the antenna coupling perspective. As the FDSM uses only a subset of its antennas at each communication step, the idea presented and studied in this paper is to harvest RF energy through the antenna subset which is not involved in the FDSM communication.

The remainder of the paper is organized as follows. In Section II, we are going to describe the architecture of the proposed system. We will study an array of four antennas in simulation with ADS to compute the mutual coupling between all the antennas. In Section III we are going to present the results of our simulations. In section IV, we give an interpretation and an analysis of the simulation results on the available power for the RF energy harvesting, and on the level of self-interference for the FDSM. Section V concludes the paper.

II. FDSM AND RFEH SYSTEM MODEL

In FDSM-RFEH, each node has N_t antennas. Unlike other MIMO systems, the SM technique activates only one transmitting antenna at each symbol period. The index of the active antenna supports additional information. The bits to be sent are grouped into frames of length: $\log_2(M) + \log_2(N_t)$, where M is the modulation order, and N_t is the number of antennas. The first $\log_2(N_t)$ are used to choose the index of the antennas that are going to send the signal. The remaining $\log_2(M)$ bits are sent by using a classical modulation scheme (ex. M-QAM). At the receiver side, we detect both the signal and the index of the activated antennas. To implement the full-duplex principle in SM, the reception of the signal from the other remote node is performed by a subset of antennas that are not used for emission. The self-interference (SI) is mainly the signal sent by the transmitting antenna of the same node to its receiving ones and an SI cancellation need to be implemented. There are different levels to perform the SIC: antenna isolation, cancellation in the analog domain, cancellation in the digital domain.

The idea behind the RFEH is to convert a RF signal into a DC one. There are five stages in a RFEH system: the propagation channel, the source of the RF signal, the impedance matching, the rectifier, and the load. The main block is the rectifier that performs the conversion of the RF signal into a DC voltage. The performance of the rectifier is characterized by its efficiency, which is the ratio between the output DC power (P_{out}), and the input RF signal power (P_{in}). For a given rectifier topology, the efficiency varies with the power level of the input RF signal and with its load.

In our system, we combine the three techniques. The specificity of our proposed RF architecture is that it harvests the RF energy from the SI generated by its own transmitting antenna in complement to the energy from the RF ambient sources. The antennas are connected to the processing chains by an intermediate functional block. This intermediate block is mainly composed of RF switches and circulators. The

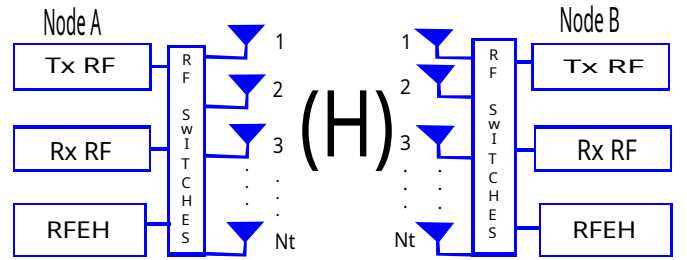


Fig. 1. Architecture of the system that combines the full-duplex spatial modulation (FDSM) and the RF energy harvesting (RFEH). Each node has N_t antennas and three processing blocks such as the transmitter T_x , the receiver R_x and the RFEH blocks.

functional architecture of the system FDSM-EH is depicted in Fig. 1.

Depending on the information to be transmitted, a subset of antennas is activated according to the SM principle. The remainder subset of antennas is used either to receive signal from a remote node or to harvest RF energy. The same process is then repeated at each symbol period T_s . The role of each antenna is different at each symbol period.

We are going to study an array of four patch antennas, as shown in Fig. 2, to analyse the power level that we can expect to harvest and the level of the self-interference to be cancelled.

III. SIMULATION RESULTS FOR AN ARRAY OF FOUR PATCH ANTENNAS

In order to perform the aforementioned study, the antenna array was designed on a Rogers RT Duroid 6006 substrate. The relative permittivity (ϵ_r) is 6.15 and the loss tangent is 0.0012. The dimensions of the antennas are summarized in Table I. All simulations are performed using the ADS Momentum software.

A. Reflection coefficient of one individual antenna

The antennas are designed to have a 50Ω input impedance at 868 MHz. In Fig. 3, the variation of the reflection coefficient S_{11} of one individual patch over the frequency is depicted.

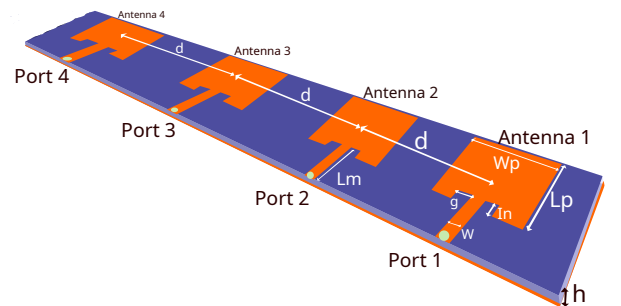


Fig. 2. The linear array of four patch antennas, simulated in Keysight's ADS Momentum software. The antennas are designed on a Rogers RT Duroid 6006 substrate. The spacing d is the distance between the centers of the patches.

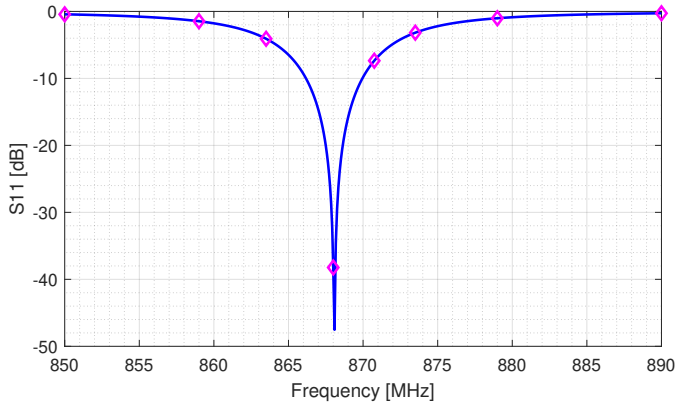


Fig. 3. Variation of the reflection coefficient for one single patch antenna versus the frequency. The antenna is matched to have $Z_e = 50 \Omega$, at the frequency 868 MHz. The reflection coefficient is minimum at the desired frequency.

As we can remark, the reflection coefficient is minimal at the desired frequency with a -10 dB bandwidth of 4 MHz.

B. Transmission coefficient between the elements of the array

Now, we are going to study an array of four identical patch antennas of the type previously presented. The impact of the spacing d between the antennas on the transmission coefficient S_{ij} , is computed. The results of the simulation are depicted in Fig. 4. The transmission coefficients are decreasing when the spacing between the antenna elements grows. The spacing d is normalised by the wavelength λ . When d is equal to

TABLE I
DIMENSIONS OF THE ANTENNA

Length L_p	69.57 [mm]
Width W_p	91.40 [mm]
Length feeding line L_m	42.40 [mm]
Width feeding line W	1.1 [mm]
Depth of slots l_n	19 [mm]
Gap on each side of the feeding line g	3.65 [mm]
Wavelength λ	345.6 [mm]

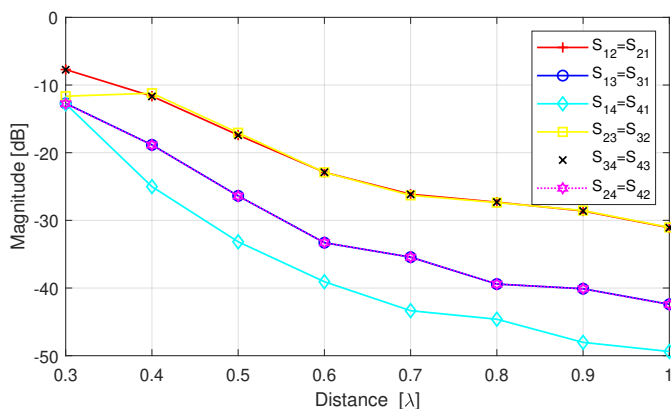


Fig. 4. Variation of the transmission coefficients, S_{ij} , between the elements of the array versus the spacing d . The distance was normalized to the wavelength λ

0.3, all the S-parameters are close to each other. The highest value is $S_{12} = -7$ dB and the least is $S_{14} = -12$ dB. The transmission coefficient is higher when the antenna is close to the transmitting antenna. S_{12} is always greater than S_{13} and S_{14} for all the values of d . When d grows, the gap between the coefficients grows also. When $d = 1$, we have $S_{12} = -31$ dB and $S_{14} = -49$ dB. Except for $d = 0.3$, one can remark that $S_{12} = S_{34}$ and $S_{24} = S_{13}$. The antenna arrays have a symmetric behaviour. We are going to interpret the impact of this result in our study of the FDSM-RFEH in the next section.

IV. INTERPRETATION OF THE SIMULATION RESULTS ON THE FDSM-RFEH SYSTEM

A. Available power via self-recycling

In FDSM-RFEH, the principle of RF power self-recycling consists of harvesting the power transferred by its own transmitting antenna to its other antennas. If an antenna is active for the transmission, a rectifier is connected to the port of another antenna. Based on the transmission coefficients, one can compute the available power that can be harvested. Let assume that the power emitted by the active antenna is 20 dBm. As each antenna has an equal probability to be used for the emission, we consider all the possible scenarios. We denote by Tx the active transmitting antenna, by Pin_{AntN} the power level at the antenna N. The results, depicted in Fig. 5, were obtained.

As a consequence of the symmetric behaviour of the array, there are two possibilities: the first case is that an antenna of the side of the array is active ($\text{Tx} = 1$ or $\text{Tx} = 4$); the second case is that one of the antennas at the middle is active ($\text{Tx} = 3$ or $\text{Tx} = 2$). We selected $\text{Tx} = 1$ for the first case and $\text{Tx} = 2$ for the second case in our study. Therefore, because of the symmetry, we can transpose the results for $\text{Tx} = 4$ and $\text{Tx} = 3$. If the antennas are close to each other, the received power level is above 0 dBm. If $\text{Tx} = 1$, the available power Pin_{Ant2} is the highest. Unlike, if $\text{Tx} = 2$, the power levels Pin_{Ant1} and Pin_{Ant3} are almost equal.

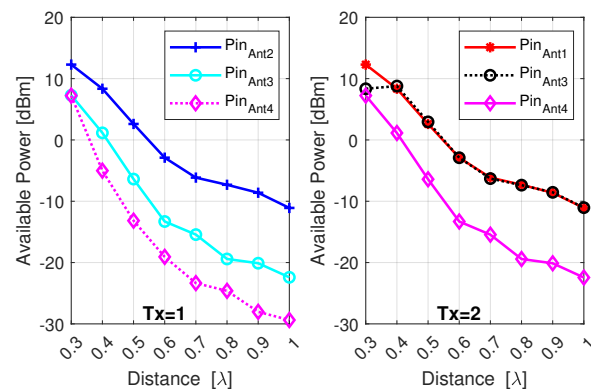


Fig. 5. Available power at the ports of the other antennas, if $\text{Tx} = 1$ on the left, $\text{Tx} = 2$ on the right. The power at the antenna number N is denoted by Pin_{AntN}

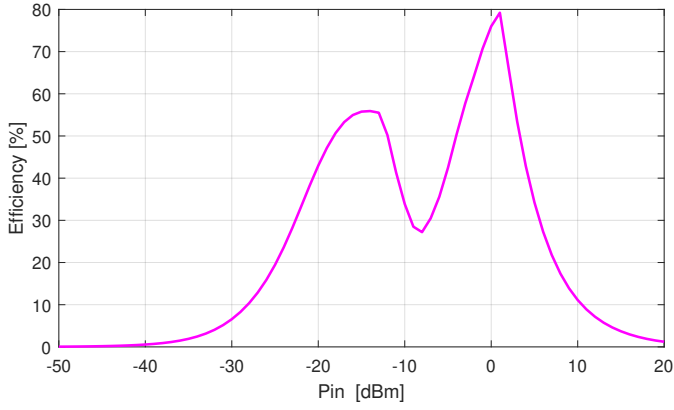


Fig. 6. Impact of the RF signal power on the efficiency of the rectifier. The input impedance is $Z_{in} = 50 \Omega$, and the load impedance is $Z_{Load} = 20 k\Omega$

Compared to the scenario in which the energy is harvested from the ambient RF sources, which are usually less than -25 dBm/cm^2 [7] in the 900 MHz band, in our case, there is more available power. As the power level changes with d , we need to use a rectifier that can operate in different power levels.

B. Expected DC-power at the output of the rectifier

Now, let assume that the rectifier proposed in [13] is used to perform the RFEH because it can operate on a wide range of input powers. The efficiency of this rectifier changes according to the power level of its input RF signal, as illustrated in Fig.6. The rectifier is matched to a 50Ω impedance at its input. For the range $[-25;7] \text{ dBm}$, the efficiency is greater than 30% and one can harvest energy even if the available power is less than -20 dBm .

$P_{Out_{AntN}}$ denotes the DC-power at the output of the rectifier connected to the antenna N and Ex denotes the antenna used to perform the RFEH. The impact of the spacing d on the expected DC-power is depicted in the Fig.7. As in the previous

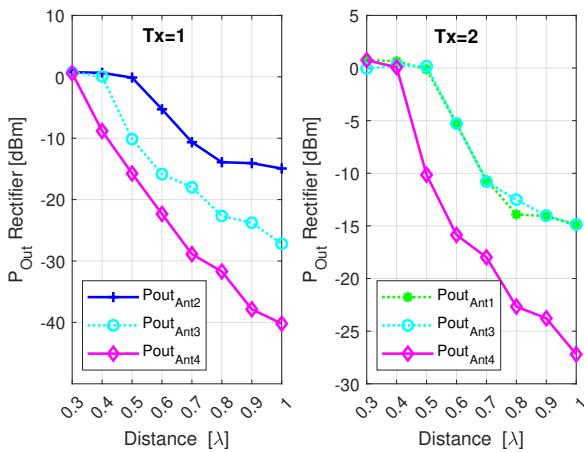


Fig. 7. Expected DC power at the output of the rectifier, when $Tx = 1$ on the left, $Tx = 2$ on the right. The output power of the rectifier connected to the antenna N is denoted by $P_{Out_{AntN}}$, and the load impedance is $Z_{Load} = 20 k\Omega$

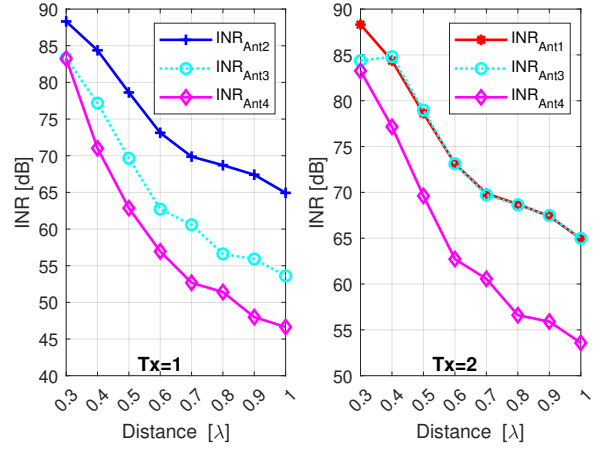


Fig. 8. Interference to noise ratio when $E_b/N_0 = 20 \text{ dB}$, $Tx = 1$ on the left, $Tx = 2$ on the right, INR_{AntN} is the INR at the antenna N

case, two scenarios are considered. If $Tx = 1$, the DC-power levels with the three antennas are different. $P_{Out_{Ant2}}$ is greater than $P_{Out_{Ant3}}$ and $P_{Out_{Ant4}}$ whatever the value of d . When the spacing is 0.3λ , the difference between the levels of the three DC-power is very small. One can expect up to 0 dBm of harvested power. And when the spacing grows, the DC-power level decreases. The minimum level of power is $P_{Out_{Ant4}} = -40 \text{ dBm}$, when $d = \lambda$. The best decision is to chose $Ex = 2$ to perform the RFEH. When $Tx = 2$, $P_{Out_{Ant1}}$ and $P_{Out_{Ant3}}$ are the same whatever the value of d . The greatest power level is $P_{Out_{Ant1}} = P_{Out_{Ant3}} = 0 \text{ dBm}$ when $d = 0.3\lambda$. Unlike the first case, we can chose between $Ex = 1$ and $Ex = 3$ to perform the RFEH.

C. The self-interference at the receiver side

Rx denotes the antenna used for the reception of the signal from the remote node. Let assume that only an active analog self-interference cancellation technique is used. The accuracy of the SIC technique depends on the interference to noise ratio (INR). To compute this metric, we assume that the communication occurs with the energy per bit to noise power spectral density ratio $E_b/N_0 = 20 \text{ dB}$. We also assume that the only significant path of the interference is the direct path. In other words, the self-interference caused by the reflection from an object in the propagation environment is neglected because they are independent to the spacing between the antenna and supposed at a large distance. The considered bandwidth of the system is 20 MHz . In this case, the variation of the INR according to the spacing d is illustrated in Fig. 8.

INR_{AntN} denotes the value of the INR at the antenna N. We consider two cases as before, if $Tx = 1$ and if $Tx = 2$. For the first case, when $d=0.3\lambda$, $INR_{Ant2} = 90 \text{ dB}$. It is impossible to reduce the self-interference below the noise level because the algorithm of self-interference cancellation has about $45\text{-}50 \text{ dB}$ of mitigation [14]. From the SI cancellation point of view, the best decision is to choose $Rx = 4$ and the spacing more than 0.6λ . In the same manner, if $Tx = 2$, the best choice is to use

Rx = 4 to perform the reception of the distant node signal with a target E_b/N_0 .

V. CONCLUSION

In this paper, a system that combines the FDSM and the RFEH was proposed. The impact of the antenna array topology on the performance of the system FDSM-RFEH was studied by analysing an array of four patch antennas. The choice of the antenna used for the reception of the signal from the remote node and for the RF energy harvesting was studied. The impact of the spacing between the antenna on the transfer coefficients was investigated. Based on the simulation results, we compute the available power that we can expect to harvest by using a realistic rectifier. The impact on the level of interference of the FDSM system was also discussed. We conclude that for the energy harvesting aspect, less the spacing is, more energy can be harvested. Unlike, for the full-duplex aspect, if the antenna spacing is small, the interference is bigger, consequently the quality of the communication is degraded. Future work will focus on the experimental part to confirm the simulation results by using a prototype of the antenna array.

REFERENCES

- [1] R. Mesleh, H. Haas, C. W. Ahn, and S. Yun, "Spatial Modulation – OFDM," *International OFDM Workshop*, 2006.
- [2] M. Di Renzo and H. Haas, "Performance Analysis of Spatial Modulation (SM)," in *IEEE International Conference on Communications and Networking in China*, pp. 1–7, 2010.
- [3] P. Yang, M. Di Renzo, Y. Xiao, S. Li, and L. Hanzo, "Design Guidelines for Spatial Modulation," *IEEE Communications Surveys Tutorials*, vol. 17, no. 1, pp. 6–26, 2015.
- [4] B. Jiao, M. Wen, M. Ma, and H. V. Poor, "Spatial Modulated Full Duplex," *IEEE Wireless Communications Letters*, vol. 3, no. 6, pp. 641–644, 2014.
- [5] Y. Zhou, F. Hutu, and G. Villemaud, "Full Duplex Spatial Modulation System Performance Depending on Self-interference Cancellation Accuracy," in *2020 14th European Conference on Antennas and Propagation (EuCAP)*, pp. 1–5, 2020.
- [6] Y. Zhou, F. Hutu, and G. Villemaud, "Full Duplex Spatial Modulation System in presence of IQ imbalance," in *2020 XXXIIIrd General Assembly and Scientific Symposium of the International Union of Radio Science*, pp. 1–3, 2020.
- [7] R. K. Sidhu, J. Singh Ubhi, and A. Aggarwal, "A Survey Study of Different RF Energy Sources for RF Energy Harvesting," in *2019 International Conference on Automation, Computational and Technology Management (ICACTM)*, pp. 530–533, 2019.
- [8] S. Hemour and K. Wu, "Radio-Frequency Rectifier for Electromagnetic Energy Harvesting: Development Path and Future Outlook," *Proceedings of the IEEE*, vol. 102, pp. 1667–1691, 2014.
- [9] A. Fumtchum, P. Tsafack, F. D. Hutu, G. Villemaud, and E. Tanyi, "A Survey of RF Energy Harvesting Circuits," *International Journal of Innovative Technology and Exploring Engineering*, vol. 10, no. 7, pp. 99–106, 2021.
- [10] M. A. Ullah, R. Keshavarz, M. Abolhasan, J. Lipman, K. P. Esselle, and N. Shariati, "A Review on Antenna Technologies for Ambient RF Energy Harvesting and Wireless Power Transfer: Designs, Challenges and Applications," *IEEE Access*, vol. 10, pp. 17231–17267, 2022.
- [11] G. Zheng, I. Krikidis, C. Masouros, S. Timotheou, D.-A. Toumpakaris, and Z. Ding, "Rethinking the Role of Interference in Wireless Networks," *IEEE Communications Magazine*, vol. 52, no. 11, pp. 152–158, 2014.
- [12] A. Koc, I. Altunbas, and E. Basar, "Two-way full-duplex spatial modulation systems with wireless powered af relaying," *IEEE Wireless Communications Letters*, vol. 7, no. 3, pp. 444–447, 2017.
- [13] J. Argote-Aguilar, F.-D. Hutu, G. Villemaud, M. Gautier, and O. Berder, "Efficient Association of Low and High RF Power Rectifiers for Powering Ultra-Low Power Devices," in *2022 29th IEEE International Conference on Electronics, Circuits and Systems (ICECS)*, pp. 1–4, 2022.
- [14] R. Askar, T. Kaiser, B. Schubert, T. Haustein, and W. Keusgen, "Active self-interference cancellation mechanism for full-duplex wireless transceivers," in *2014 9th International Conference on Cognitive Radio Oriented Wireless Networks and Communications (CROWNCOM)*, pp. 539–544, 2014.